Assessment of the metabolic activity of bone grafts with ^{18}F-fluoride PET

Winfried Brenner[1], Cheryl Vernon[1], Ernest U. Conrad[2], Janet F. Eary[1]

[1] Division of Nuclear Medicine, University of Washington Medical Center, Seattle, USA
[2] Department of Orthopaedics, University of Washington Medical Center, Seattle, USA

Abstract. *Purpose:* The aims of this prospective study were to evaluate quantitative approaches to ^{18}F-fluoride positron emission tomography (PET) imaging in allogenic bone grafts of the limbs, and to assess the time course of graft healing after surgery. *Methods:* We performed a total of 52 dynamic ^{18}F-fluoride PET studies in 34 patients with cancellous and full bone grafts. Seven patients were imaged three times at 6, 12, and 24 months after surgery, and four patients were imaged twice. PET data were quantitatively analyzed using non-linear regression (NLR) analysis, Patlak analysis, and standardized uptake value (SUV). *Results:* Fluoride bone metabolism in cancellous grafts decreased by 25% from 6 to 12 months post surgery, and revealed a total decrease of 60–65% after 2 years for SUV, K_{Pat}, and K_{NLR}. Full bone grafts first showed an increase by 20% from 6 to 12 months and from then on decreased to 70% of the initial activity at the end of 2 years with either quantification method. In two patients with non-union of their full bone grafts, increases in SUV, K_{Pat}, K_{NLR}, and K_1 far above average and outside the normal time pattern were observed. Highly significant correlations were found between SUV, K_{Pat}, K_{NLR}, and K_1 for both grafts and normal limb bones. In patients imaged repeatedly, the percentage changes in fluoride graft metabolism were also significantly correlated between SUV, K_{Pat}, and K_{NLR}. *Conclusion:* Quantitative ^{18}F-fluoride PET is a promising tool for assessment of fluoride metabolism and normal healing in bone grafts of the limbs.

Keywords: ^{18}F-fluoride ion – Positron emission tomography – Bone grafts – Bone metabolism

Winfried Brenner (✉)
Division of Nuclear Medicine,
University of Washington Medical Center, 1959 NE Pacific Street,
P.O. Box 356113, Seattle, WA 98195-6113, USA
e-mail: winbren_2000@yahoo.com
Tel.: +1-206-5984235, Fax: +1-206-5984496

Introduction

In a variety of benign and malignant bone tumors of the limbs, allogenic bone grafts are used for replacement of the resected bone to maintain stability and functional integrity. In benign tumors with limited resection of bone as well as in small malignant tumors, the resection cavity is often small enough to be filled in with cancellous chip bone grafts. Massive full bone grafts are used for replacement if whole parts of the bone have to be resected to completely remove the tumor with clear margins. Complication rates due to infection or, more commonly, non-union and fractures of the grafts are especially high in full bone grafts. These occurrences are even higher in tumor patients receiving adjuvant chemotherapy and/or radiation, with complication rates of 40–68% [1, 2].

To assess bone graft healing during follow-up, clinical examination and X-ray are the most widely used and accepted tools. However, plain radiography is unreliable in the early prediction of impaired graft healing because it assesses morphologic signs such as gaps at junction sites, callus formation, and bridging bone formation, which occur late in the normal course of healing [3]. Since other imaging techniques such as computed tomography, magnetic resonance imaging, or bone scintigraphy are even less accepted or standardized, imaging assessments for bone allografts are controversial [2, 4, 5]. Due to this lack of reliable imaging methods to assess graft healing, decisions regarding graft removal in cases of non-union are usually made rather late, based on pain, restricted movement, and other clinical symptoms, or on radiologic signs of complications such as graft fractures or missing callus formation and bridging.

^{18}F-fluoride positron emission tomography (PET) has the potential to exactly measure fluoride bone metabolism in specific spatial regions [6–11]. A few reports on ^{18}F-fluoride PET have shown that this technique can provide

metabolic information which may serve as a potential measure of bone graft remodeling and healing [12–16].

The aims of this study were to systematically evaluate ^{18}F-fluoride PET imaging in allogenic bone grafts of the limbs with respect to different quantification methods such as non-linear regression (NLR) analysis, Patlak graphical analysis, and standardized uptake value (SUV), to assess the time course of graft healing during the first 2 years after surgery, and to compare fluoride bone metabolism in different types of graft, i.e., cancellous and full bone grafts.

Materials and methods

Patients

For this study, 34 consecutive patients presenting for regular follow-up examinations after bone graft surgery were selected for dynamic ^{18}F-fluoride imaging. The patients ranged in age from 18 to 66 years and had a wide range of benign (*n*=19) and malignant (*n*=15) tumors of limb bones. Grafts, either cancellous chips (*n*=23) or full bone grafts (*n*=11), were located in the humerus (*n*=13), in the femur (*n*=12), in the tibia (*n*=6), in the fibula (*n*=1), or in the bones of the foot (*n*=2). None of the patients showed any evidence of residual tumor tissue or local relapse at the time of scanning. Only one patient with a Ewing sarcoma received chemotherapy between imaging at 6 and 12 months after surgery. All patients had serum creatinine levels within the normal range, indicating normal kidney function. Imaging was performed at 2–51 months (mean 13 months) after graft surgery. Seven patients were imaged three times, and four patients were imaged twice after surgery, resulting in a total of 52 ^{18}F-fluoride PET scans. Patients gave informed consent for the PET studies by signing forms approved by the University of Washington Human Subjects and Radiation Safety Committees.

PET imaging

Imaging studies were performed on an Advance Tomograph (General Electric Medical Systems, Waukesha, WI) operating in a two-dimensional high-sensitivity mode, with 35 imaging planes (plane thickness 4.25 mm) per axial field of view of 15 cm. An intravenous line was placed in each arm, one side for the tracer injection, the other side for venous blood sampling. After the patients had been positioned in the tomograph, a 25-min attenuation scan over the graft site was acquired. A standard activity of 3.7 MBq/kg body weight of ^{18}F-fluoride ion, produced according to the United States Pharmacopeia guidelines, was dissolved in 10 ml of 0.9% saline solution and infused over 2 min with a syringe pump. Simultaneously with the beginning of tracer infusion, a 60-min dynamic sequence of 24 emission scans was started with four 20-s, four 40-s, four 1-min, four 3-min, and eight 5-min frames. Serial venous blood samples were obtained at 1-min intervals up to 10 min after injection, followed by five samples at 2-min intervals and eight samples at 5-min intervals. Although venous blood sampling tends to overestimate fluoride bone flux by approximately 5% due to a systematic underestimation of blood activity [17], we applied simple venous sampling in order to keep the methodological effort as low as possible for routine use in a clinical setting. Blood samples were centrifuged, and plasma was counted on a Cobra well counter (Packard Instrument Co., Meriden, CT).

All images underwent corrections for random and scattered coincidence events. Each image of the dynamic dataset was corrected for attenuation and physical decay of ^{18}F-fluoride. Images were reconstructed onto 128×128 matrices by filtered back-projection using a Hanning filter, resulting in a reconstruction resolution of approximately 12 mm for the dynamic images [18, 19]. Cross-calibration of image data with blood sample counts was performed on the same day of each study using a 500-ml vial containing a known amount of ^{18}F-fluoride.

Data analysis

PET data were analysed by a region of interest (ROI) technique. The 30- to 60-min summed images were used to guide ROI placement. Circular or elliptic ROIs, ranging in size from 9 to 30 pixels equaling 1.7–4.4 cm^2, were placed over the midshaft contact zone between the graft and the original bone including the area with maximum counts (Fig. 1). This region was chosen because the shaft end is the common region of non-union rather than the epi-/metaphyseal end of the graft. Each ROI was applied to five or six contiguous planes in each frame, creating a volume of interest (VOI). A VOI of the same size was used on the contralateral side as a reference volume for normal bone tissue. Tissue time-activity curves (TAC) were generated for the graft and the contralateral normal bone from application of the VOIs to the whole dynamic image set. These data were then processed using both NLR and Patlak graphical analysis. The same VOIs were used for calculating SUVs.

Standardized uptake value. SUV was calculated according to the following formula:

$$SUV = \frac{A}{ID/m}$$

where *A* is the mean tissue activity within the VOI in summed images from 30 to 60 min of the dynamic data set, ID is the injected dose, and *m* is the patient's body weight.

Fig. 1a, b. Coronal views of summed images from 30 to 60 min at 6 months after surgery depicting schematically the VOIs in **a** a patient with a cancellous graft of the proximal humerus and **b** a patient with a full bone graft in the distal femur
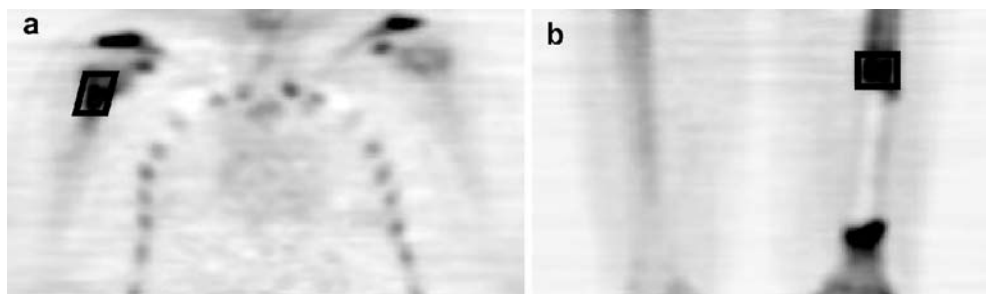
Patlak analysis. The fluoride bone influx rate was calculated using Patlak graphical analysis [20, 21] assuming a three-compartment model as described by Hawkins et al. [6]. In Patlak analysis, the fluoride bone influx rate K_{Pat} is determined by the following equation:

$$\frac{C_I(t)}{C_b(t)} = \frac{K_{Pat}\left[\int_0^t C_b(t)dt\right]}{C_b(t)} + V$$

where $C_I(t)$ is the activity concentration at time t measured using the ROI approach, $C_b(t)$ is the blood concentration of tracer, and V is the effective distribution volume of the tracer. K_{Pat} is the net uptake of fluoride in the bone assuming that fluoride is irreversibly bound to the bones (k_4=0). K_{Pat} is obtained from the slope of the linear part of the fit of $C_I(t)/C_b(t)$ vs $[\int_0^t C_b(t)dt]/C_b(t)$.

The linear portion of the curve was usually observed from 10 to 50 min after injection. These times or, if necessary, individually adjusted times were used as the boundaries for the graphical fit to estimate K_{Pat}. For the fit, the time for each point in the tissue TAC was taken as the center of the time bin. Matched time points in $C_b(t)$ were obtained using linear interpolation between neighboring time points in the measured blood curve.

Non-linear regression. NLR analysis was also performed on the basis of a three-compartment model consisting of the plasma space, an unbound and a bound bone compartment as described by Hawkins et al. [6]. The rate constants K_1 to k_4 describe the transport of fluoride between the compartments: K_1 and k_2 for the forward and reverse transport from plasma to the unbound interstitial bone compartment, k_3 for binding to bone apatite and k_4 for the release from the mineral bone compartment. A fifth parameter for the fractional blood volume (fBV) was included to account for the contribution of non-extracted tracer in the vascular space to the measured tissue data. The delay of tracer arrival in the bone tissue was optimized by chi-square fitting in each patient for each region. The blood input function and the TAC data were fitted to this compartment model using an NLR algorithm (PMOD 2.00, PMOD Group, University Hospital Zurich, Switzerland) estimating the kinetic parameters K_1 to k_4, and fBV. The fluoride bone influx rate K_{NLR} is the net forward transport parameter calculated as:

$$K_{NLR} = K_1 k_3 / (k_2 + k_3)$$

Statistical analysis

Results are given as mean ±1 standard deviation (SD). For each patient the graft values for SUV and K_{Pat} were plotted against K_{NLR}, and the Spearman's rank correlation coefficient was calculated using a spreadsheet program (Excel, Microsoft Corp., Redmond, WA). The strength of the correlation was judged by the correlation coefficient. Student's t test or ANOVA was used to evaluate statistical differences between subgroups with $p<0.05$ considered to be statistically significant. Tests for paired data sets were used to test for differences between time points or graft and normal bones within a patient group, while tests for unpaired data sets were used to evaluate differences between different patient groups, e.g., based on graft types. In patients imaged repeatedly, changes of graft metabolic rates were expressed as percentages of the initial values. In order to account for variations in bone activity due to normal changes over time, we calculated graft-to-contralateral normal bone ratios to describe changes in kinetic parameters of bone grafts over time and compare differences between the two graft types and normal limb bones.

Results

Fluoride bone metabolic values and NLR rate constants for bone grafts and contralateral normal limb bones are summarized in Table 1. Significant differences between graft and normal bone values (lumped values of all three time points of imaging), with elevated values in bone grafts, were observed for SUV, K_{Pat}, and K_{NLR} as well as for all NLR rate constants and fBV except k_4.

In patients imaged repeatedly, the relative changes in fluoride bone metabolic values (n=18) of the normal limb bones in percent of the initial value were

Table 1. SUV, K_{Pat}, and NLR ^{18}F-fluoride metabolic parameters for bone grafts and contralateral normal limb bones

	SUV	K_{Pat} (ml/min/ml)	K_{NLR} (ml/min/ml)	K_1 (ml/min/ml)	k_2 (min^{-1})	k_3 (min^{-1})	k_4 (min^{-1})	fBV (ml/ml)
Grafts								
Mean	5.1	0.0328	0.0347	0.0804	0.1678	0.1239	0.0056	0.0764
SD	2.4	0.0171	0.0176	0.0398	0.1121	0.0750	0.0055	0.0794
Min.	1.6	0.0084	0.0079	0.0158	0.0366	0.0239	0	0
Max.	12.6	0.0792	0.0751	0.2058	0.4898	0.3725	0.0256	0.4255
Normal bones								
Mean	1.3	0.0079	0.0081	0.0224	0.1224	0.0741	0.0051	0.0363
SD	0.8	0.0045	0.0048	0.0124	0.0753	0.0497	0.0055	0.0380
Min.	0.4	0.0035	0.0027	0.0047	0.0100	0.0171	0	0
Max.	4.4	0.0256	0.0278	0.0765	0.3916	0.2940	0.0213	0.1596
P value	<0.001	<0.001	<0.001	<0.001	0.018	<0.001	0.646	0.002
Ratio[a]	3.9	4.2	4.3	3.6	1.4	1.7	1.1	2.1

[a] Ratio, mean graft value divided by mean normal bone value

Table 2. Graft-to-normal ratios for SUV, K_{Pat}, and K_{NLR} at 6, 12, and 24 months after surgery

Pts	SUV			K_{Pat}			K_{NLR}		
	6 months	12 months	24 months	6 months	12 months	24 months	6 months	12 months	24 months
Cancellous chips grafts									
1	2.9	2.3		3.2	2.3		3.5	2.4	
2	5.2	3.2	1.6	7.0	3.9	2.0	7.1	5.0	2.1
3	7.6	4.3	2.1	7.8	4.6	2.0	8.2	4.8	2.3
4	12.5	7.4	8.5	12.1	6.9	5.1	13.7	6.7	5.7
5	3.0	3.0		3.5	3.2		3.7	3.1	
6	2.7	1.6		2.7	1.7		2.8	1.8	
Mean	5.6[a]	3.6[a]	4.1	6.1[a]	3.8[a,b]	3.0[b]	6.5[a]	4.0[a]	3.4
Full bone grafts									
7	4.0	4.6	**5.5**	4.1	4.8	**6.5**	3.4	5.3	**6.0**
8	3.6	4.0	2.5	4.2	4.4	2.6	4.4	5.6	3.5
9	3.6	4.5	3.1	3.8	4.1	3.2	3.9	4.5	3.5
10	4.5	**8.5**		4.5	**8.6**		4.5	**8.1**	
11	1.8	2.3		1.9	2.4		1.9	2.7	
Mean	3.3[a]	3.9[a]	2.8	3.5[a]	3.9[a]	2.9	3.4[a]	4.5[a]	3.5

Numbers in bold represent patients with non-union of the grafts; these values were excluded from calculations of the mean and paired Student's *t*-test

[a] Significant differences between 6 and 12 months ($p<0.05$)
[b] Significant differences between 12 and 24 months ($p<0.05$)

0.4%±25.1% for SUV, −0.1%±12.7% for K_{Pat}, and −5.2%±12.8% for K_{NLR}. Changes were randomly scattered in both negative and positive directions as indicated by mean values close to zero, suggesting no major shifts in normal bone activity over time for these patients.

Grafts showed a different behavior over time in patients imaged repeatedly. Uptake in cancellous bone grafts decreased from 6 to 12 months post surgery by approximately 25%, and revealed a total decrease of 60–65% for SUV, K_{Pat}, and K_{NLR} after 2 years (Fig. 2). Full bone grafts, on the other hand, showed an increase in fluoride bone metabolism by approximately 20% from 6 to 12 months with either quantification method. From then on, fluoride bone metabolism decreased to 70% of the initial activity at the end of 2 years (Fig. 2).

In cancellous bone grafts, a significant decrease in the graft-to-normal ratio of bone activity was observed from 6 to 12 months and from 6 to 24 months after surgery for all three parameters, SUV, K_{Pat}, and K_{NLR}. From 12 to 24 months, only Patlak values decreased significantly while SUV ($p=0.455$) and K_{NLR} ($p=0.073$) did not reach significance (Table 2). K_1 was the only NLR rate constant which reached significance after 24 months, while k_2–k_4 and fBV did not show uniform trends over time (Table 3). In comparing the kinetic parameters of cancellous bone grafts with the contralateral normal side in each patient, we found lower k_4 values in grafts than in contralateral normal bones, resulting in graft-to-normal ratios <1 in most of the patients, while for all the other
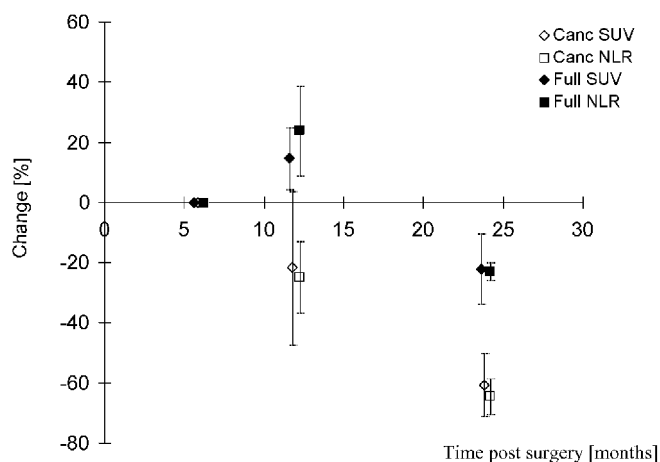

Fig. 2. Percentage change of SUV and K_{NLR} in cancellous (*Canc*) and full (*Full*) bone grafts up to 2 years after surgery. Results are mean±SD ($n=3$–6)

parameters the graft values were usually higher than the corresponding normal values up to 2 years, as indicated by ratios >1 (Table 3). These differences were significant for K_1 ($p<0.001$) and k_3 ($p=0.027$).

In full bone grafts, a significant increase in the graft-to-normal ratio was obtained for SUV, K_{Pat}, and K_{NLR} during the time from 6 to 12 months after surgery (Table 2). Although the increase in graft metabolism from 6 to 12 months was followed by a decline from 12 to 24 months to below the initial values at 6 months in two patients with normal graft healing, this decline was

Table 3. Graft-to-normal ratios for NLR rate constants at 6, 12, and 24 months after surgery

Pts	K_1			k_2			k_3			k_4			fBV		
	6 months	12 months	24 months	6 months	12 months	24 months	6 months	12 months	24 months	6 months	12 months	24 months	6 months	12 months	24 months
Cancellous chips grafts															
1	2.4	2.6		1.3	4.6		2.5	4.1		0.5	0.6		1.1	0.1	
2	4.0	3.2	2.3	2.2	2.6	3.8	5.2	5.1	3.5	–	–	–	0.1	0.4	0.1
3	4.0	4.9	2.9	0.2	1.5	2.1	0.7	1.5	1.3	1.0	–	1.8	7.2	4.0	2.1
4	7.7	6.5	6.9	1.1	0.7	1.2	2.5	0.7	0.7	0.4	0.2	0.4	–	5.1	0.2
5	2.5	1.9		0.6	0.3		0.9	0.8		0.1	0.1		1.2	0.1	
6	3.3	1.4		2.3	1.0		1.7	1.4		0.5	1.0		0.8	0.9	
Mean	4.0[a]	3.4	4.1[a]	1.3	1.8	2.4	2.2	2.2	1.8	0.5	0.5	1.1	2.1	1.8	0.8
Full bone grafts															
7	3.1	2.3	**4.6**	0.6	0.4	**1.6**	0.7	1.5	**2.6**	0.1	–	–	3.7	–	**2.9**
8	4.7	4.3	2.5	1.4	1.7	2.0	1.3	2.5	3.2	0.1	10.9	–	8.4	3.8	2.6
9	3.7	4.6	3.4	1.1	1.0	2.4	1.3	0.9	2.5	0.8	1.1	1.4	2.2	3.7	0.6
10	7.3	**14.6**		3.1	**32.9**		1.2	**7.1**		–	–		5.2	**8.3**	
11	2.8	2.6		4.1	1.3		2.1	1.4		1.6	–		0.9	3.5	
Mean	3.6	3.4	2.2	1.8	1.1	2.2	1.4	1.6	2.9	0.6	4.0	1.4	3.8	2.8	1.6

Numbers in bold represent patients with non-union of the grafts; these values were excluded from calculations of the mean and paired Student's *t* test

–, A ratio could not be calculated because one of the rate constants was zero

[a] Significant differences between 6 and 24 months in patients 2, 3, and 4 ($p<0.05$)

statistically not significant owing to the low number of subjects. As already observed in cancellous bone grafts, K_1 ($p<0.001$), k_2 (NS), k_3 ($p=0.015$), and fBV ($p=0.002$) were generally higher in full bone grafts than in the contralateral normal bones. k_4 yielded both lower and higher values in grafts, resulting in graft-to-normal ratios both below and above 1, and the differences between grafts and normal bones therefore were not significant (Table 3).

Despite these different time courses of bone metabolism, we did not find significant differences between metabolic parameters or single NLR rate constants of cancellous and full bone grafts at the different time points after surgery. Interestingly, however, the mean graft-to-normal ratios of SUV, K_{Pat}, and K_{NLR} at 6 months were all lower, though not significantly so, in full bone grafts, while this pattern changed at 1 year after surgery. At that time point, full bone grafts showed higher values for all three parameters, the differences again being non-significant (Table 2). These findings are in line with the different time courses of bone activity patterns in cancellous and full bone grafts.

Non-union of the grafts was diagnosed in patients 7 and 10 with full bone grafts at 13 and 19 months after surgery, respectively, and both patients underwent PET imaging immediately prior to revision surgery (Tables 2, 3). Both patients showed an increase in fluoride bone metabolism and bone blood flow. In patient 7, increases of 20–30% in the graft-to-normal ratios were observed

for SUV, K_{Pat}, and K_{NLR} from 13 to 19 months after initial graft surgery, instead of the usual decreases observed in cases of normal healing. K_1 increased by 50%. In patient 10, increases of 80–90% in graft-to-normal ratios for SUV, K_{Pat}, and K_{NLR} were seen from 7 to 13 months after initial surgery, and K_1 increased by 50%. These changes were significantly higher than the mean increase in these parameters of approximately 20% that is usually associated with uncomplicated healing. For k_2 to k_4 and fBV no specific patterns in comparison with healing grafts were found.

In comparing the different quantification methods in terms of fluoride bone uptake for both grafts and normal limb bones, we found highly significant correlations ($p<0.01$ each) between SUV and K_{NLR} (grafts, $r=0.84$; normal bones, $r=0.91$), K_{Pat} and K_{NLR} (grafts, $r=0.99$; normal bones, $r=0.99$), and K_{NLR} and K_1 (grafts, $r=0.88$; normal bones, $r=0.78$). There was no correlation between K_{NLR} and k_3, either for grafts or for contralateral normal limb bones. In patients imaged repeatedly, the percentage changes in fluoride metabolism of the grafts were also significantly correlated ($n=18$; $p<0.01$ each) for SUV and K_{Pat} ($r=0.96$), SUV and K_{NLR} ($r=0.91$) (Fig. 3a), and K_{Pat} and K_{NLR} ($r=0.97$) (Fig. 3b). Only in one patient with a cancellous bone graft did SUV show an increase of 17.4% from 7 to 12 months after surgery while both K_{Pat} (−11.8%) and K_{NLR} (−13.8%) decreased.
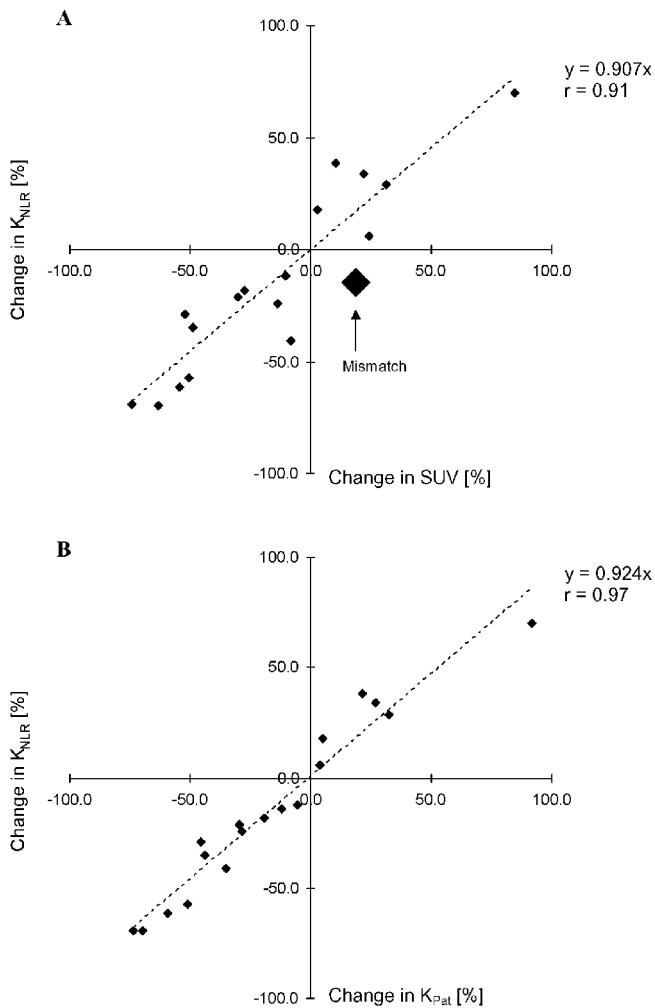
A

B

Fig. 3. Correlation of percentage change in graft fluoride metabolism between **a** SUV and K_{NLR}, and **b** K_{Pat} and K_{NLR}

Discussion

First reports on ^{18}F-fluoride PET in a limited number of patients have shown that this technique has the potential to provide pathophysiologically relevant information on bone grafts in terms of bone metabolism and bone blood flow as calculated by compartmental NLR methods and Patlak analysis [12–14, 16]. Based on these promising data, we started ^{18}F-fluoride PET imaging in patients with allogenic bone grafts of the limbs with the aim of assessing the time course and characteristic patterns of normal and impaired graft healing. Applying SUV in addition to the compartmental modeling approach, we aimed to test an even simpler quantification tool widely used in oncology which could be easily integrated into the routine daily work of any PET center.

As already reported in literature [12–14, 16], we found a decrease in fluoride metabolism in bone grafts over a period of 2 years after surgery while the contralateral normal bones showed no significant metabolic changes during the same time. Despite this general de-

crease, however, bone metabolism at 24 months after surgery was still significantly higher in both cancellous grafts and the border zone of full bone grafts compared with normal limb bones. In cancellous bone grafts, the mean graft-to-normal ratio at that time point was 3.4 for K_{NLR}, and this ratio was in the same order of magnitude for full bone grafts (Table 2). Patlak analysis and SUV yielded comparable results. Piert et al. also observed increased bone activity after a mean follow-up of 2 years after hip augmentation surgery with cancellous grafts and explained these findings by continued stress to the normal surrounding bone [13]. This is in line with histopathological findings in cancellous grafts demonstrating bone remodeling and formation of new bone to allograft fragments in peripheral areas up to 53 months after graft implantation [4]. Similar findings were obtained in massive bone allografts, in which bone growth was observed up to 48 months after surgery in areas where the graft was in contact with viable host bone [5].

Although both types of graft investigated in our study, that is cancellous and full bone grafts, showed a decrease in fluoride bone metabolism 2 years after surgery, the time course of changes in metabolism was completely different in each (Fig. 2). In cancellous grafts, a significant stepwise decrease in bone metabolism of 25% from 6 to 12 months and of 65% at 24 months was observed. Full bone grafts, on the other hand, were characterized by an initial significant increase of 15–25%, depending on the underlying quantification method, and then a decrease of 35% between 12 and 24 months, resulting in a non-significant total decrease of 20% compared with the initial values at 6 months.

This difference in time patterns between the two graft types reflects the difference in graft features. In cancellous grafts, the small bone chips usually show relatively fast healing, resulting in clinically and radiologically stable union conditions within 1 year after surgery. A decrease in fluoride bone uptake from 6 to 24 months is therefore in line with clinical findings and represents graft biology. In full bone grafts, however, healing is usually delayed, complications occur more frequently, and non-union, based on clinical findings and X-rays, can usually be diagnosed as late as 18–24 months after surgery. This clinical experience is confirmed by histopathological findings showing ongoing graft remodeling for up to 48 months after surgery in the contact zone, whereas most of the other parts of full bone grafts show no remodeling at all [5]. This is in accordance with ^{18}F-fluoride PET findings which demonstrated decreased bone metabolism in central parts of full bone grafts, as reported in the literature [14] and shown in Fig. 1. Bone remodeling in the contact area and ingrowth of new host bone seem to increase over time, reaching a peak activity at about 1 year after surgery with subsequently decreasing bone activity.

K_1 as a marker of bone blood flow was significantly correlated with K_{NLR}, and thus, with bone metabolism.

This was to be expected according to the results of Piert and co-workers [22, 23]. The maximum flow value observed in our study was 0.21 ml/min/ml, and thus just in the lower range of critical flow values above which K_1 differs increasingly from real blood flow owing to diffusion limits of fluoride transport. Interestingly, the correlation between K_1 and K_{NLR} was better in grafts ($r=0.88$), with a mean K_1 of 0.0804 ml/min/ml, than in normal limb bones ($r=0.78$), with a mean flow value of 0.0224 ml/min/ml. Whether this is due to more robust count statistics, and, thus, more reliable modeling results in high uptake areas such as bone grafts, or whether in limb bones with low fluoride bone metabolism the coupling between blood flow and metabolism is less pronounced in general, cannot be decided decisively based on our data. Low count statistics in normal limb bones, however, seem to be the more reasonable cause.

Despite a significant coupling between bone blood flow and bone metabolism in general, changes in K_1 reached statistical significance only in cancellous grafts after 24 months, and the strictly consistent time patterns observed for K_{NLR} were not found for K_1 (Tables 2, 3). The reason for the discrepancy between K_1 and K_{NLR} is probably the higher variance of single rate constants compared with the more stable flux values [6], although different time patterns in changes of bone blood flow and bone metabolism cannot be ruled out in individual patients. Since ROIs in our study were placed over the graft/normal bone border zone, the blood flow within the ROI will have reflected not only pure bone blood flow but also blood flow to varying amounts of connective and repair tissues which do not show fluoride metabolism. This would explain a potential disconnection of the usually strong coupling of flow and metabolism in the contact zone.

Non-union of the graft was diagnosed in two patients with full bone grafts. Both patients showed a significant increase in SUV, K_{Pat}, and K_{NLR}. In one patient an increase was found from 13 to 19 months instead of the commonly observed decrease in the graft-to-normal ratio observed in cases of normal healing. In the second patient, the graft-to-normal ratio almost doubled from 7 to 13 months instead of the usual increase of 20%. In both patients K_1 doubled, indicating a highly increased blood flow. k_2 and k_3 increased significantly (Table 3), suggesting increased fluoride rediffusion to the vascular space and increased fluoride incorporation into the bone. All these changes are consistent with increased blood flow, vascular permeability, and bone turnover, as expected in the presence of inflammatory and repair mechanisms induced in the host tissue by conditions of non-union.

The different quantification methods used for assessment of fluoride metabolism in both grafts and normal limb bones were highly correlated. More important for clinical use is that the percentage changes in metabolic activity of the grafts were also highly correlated in pa-

Table 4. Correlation of percentage changes and categorized changes in SUV, K_{Pat}, and K_{NLR} for bone grafts imaged repeatedly

SUV (%)	Patlak (%)	NLR (%)	SUV	Patlak	NLR
−48.8	−44.0	−35.2	−1	−1	−1
−52.2	−45.4	−28.8	−1	−1	−1
−8.3	−35.4	−40.9	**0**	−1	−1
−10.7	−5.6	−12.1	0	0	0
17.4	−11.8	−13.8	0	0	0
−27.3	−19.3	−18.2	**−1**	0	0
−50.5	−50.9	−57.5	−1	−1	−1
−74.4	−69.6	−69.2	−1	−1	−1
−63.0	−73.5	−69.5	−1	−1	−1
−54.7	−59.2	−61.4	−1	−1	−1
−30.3	−29.7	−21.6	−1	−1	−1
−13.8	−28.8	−24.1	**0**	−1	−1
2.5	4.9	17.5	0	0	0
10.3	21.2	38.4	**0**	1	1
24.1	3.9	5.8	**1**	0	0
84.8	91.6	69.8	1	1	1
22.0	27.0	33.9	1	1	1
31.3	32.2	28.8	1	1	1

−1, decrease >20%; 0, change ≤20%; 1, increase >20%
Numbers in bold represent differing results between SUV and Patlak/NLR

tients imaged repeatedly (Fig. 3). A discrepancy between the different methods was found in only one patient with a cancellous bone graft in whom SUV increased by 17% while both K_{Pat} and K_{NLR} decreased by approximately 13% at the same time. When regarding only metabolic changes in SUV, K_{Pat}, and K_{NLR} of more than 20% as significant [24, 25], there was a complete match between K_{Pat} and K_{NLR} in all 18 grafts, while five mismatches were found each for SUV and K_{Pat}, and SUV and K_{NLR} (Table 4). Interestingly, all mismatches showed "no change" for one parameter and either an increase or decrease for the other parameter, but no case was observed in which one parameter indicated an increase while the other denoted a significant decrease. Considering NLR as the gold standard, assessment of changes in graft metabolism by means of SUV would have resulted in different ratings in five of 18 grafts when applying a 20% threshold for considering differences between two values as true changes. SUV is therefore less reliable than compartmental approaches, at least from a methodological point of view. For NLR analysis the question arises as to whether calculation of single rate constants provides relevant information in addition to K_{NLR}. K_1 is significantly coupled to K_{NLR} over a wide range of bone blood flow values, and k_2−k_4 are rather unstable parameters showing high coefficients of variation and a strong interconnection to modeling constraints. Patlak analysis, therefore, seems to yield the best trade-off between methodological effort and precise biological information: it is highly correlated to K_{NLR} but is computationally simpler than NLR.

In conclusion, Patlak-derived bone influx values of ^{18}F-fluoride and SUV were strongly correlated with K_{NLR} in bone grafts for both the absolute measures and the percentage changes over time. Applying a threshold of 20% for considering metabolic changes as significant, SUV yielded discrepant results in five out of 18 grafts while Patlak findings were identical to K_{NLR}. The time course of fluoride bone metabolism was different in cancellous chips and full bone grafts: full bone grafts showed increasing SUV, K_{Pat}, and K_{NLR} as well as K_1 as an estimate of bone blood flow from 6 to 12 months after surgery with a subsequent decrease from 12 to 24 months, while in cancellous grafts all parameters decreased continuously over the whole period. Non-union of the graft with the need for surgical intervention resulted in an increase in SUV, K_{Pat}, K_{NLR}, and K_1 far above average and outside the normal time pattern in full bone grafts. Thus, quantitative ^{18}F-fluoride PET is a promising tool for assessment of bone metabolism and healing in bone allografts.

References

1. Ortiz-Cruz E, Gebhardt MC, Jennings LC, Springfield DS, Mankin HJ. The results of transplantation of intercalary allografts after resection of tumors. A long-term follow-up study. J Bone Joint Surg Am 1997;79:97–106

2. Roebuck DJ, Griffith JF, Kumta SM, Leung PC, Metreweli C. Imaging following allograft reconstruction in children with malignant bone tumours. Pediatr Radiol 1999;29:785–793

3. Weissman BN, Pathria MN, Garfin SR. Postoperative imaging. In: Resnick D, ed. Bone and joint imaging, 2nd edn. Philadelphia: Saunders; 1996:165–182

4. Heekin RD, Engh CA, Vinh T. Morselized allograft in acetabular reconstruction. A postmortem retrieval analysis. Clin Orthop 1995;319:184–190

5. Hooten JP Jr, Engh CA, Heekin RD, Vinh TN. Structural bulk allografts in acetabular reconstruction. Analysis of two grafts retrieved at post-mortem. J Bone Joint Surg Br 1996; 78:270–275

6. Hawkins RA, Choi Y, Huang SC, et al. Evaluation of the skeletal kinetics of fluorine-18-fluoride ion with PET. J Nucl Med 1992;33:633–642

7. Messa C, Goodman WG, Hoh CK, et al. Bone metabolic activity measured with positron emission tomography and [18F]fluoride ion in renal osteodystrophy: correlation with bone histomorphometry. J Clin Endocrinol Metab 1993; 77:949–955

8. Schiepers C, Nuyts J, Bormans G, et al. Fluoride kinetics of the axial skeleton measured in vivo with fluorine-18-fluoride PET. J Nucl Med 1997;38:1970–1976

9. Cook GJ, Lodge MA, Marsden PK, Dynes A, Fogelman I. Non-invasive assessment of skeletal kinetics using fluorine-18 fluoride positron emission tomography: evaluation of image and population-derived arterial input functions. Eur J Nucl Med 1999;26:1424–1429

10. Piert M, Zittel TT, Becker GA, et al. Assessment of porcine bone metabolism by dynamic [18F]fluoride ion PET: correlation with bone histomorphometry. J Nucl Med 2001; 42:1091–1100

11. Blake GM, Park-Holohan SJ, Fogelman I. Quantitative studies of bone in postmenopausal women using ^{18}F-fluoride and ^{99m}Tc-methylene diphosphonate. J Nucl Med 2002;43:338–345

12. Berding G, Burchert W, van den Hoff J, et al. Evaluation of the incorporation of bone grafts used in maxillofacial surgery with [18F]fluoride ion and dynamic positron emission tomography. Eur J Nucl Med 1995;22:1133–1140

13. Piert M, Winter E, Becker GA, et al. Allogenic bone graft viability after hip revision arthroplasty assessed by dynamic [18F]fluoride ion positron emission tomography. Eur J Nucl Med 1999;26:615–624

14. Schliephake H, Berding G, Knapp WH, Sewilam S. Monitoring of graft perfusion and osteoblast activity in revascularised fibula segments using [18F]-positron emission tomography. Int J Oral Maxillofac Surg 1999;28:349–355

15. Emami A, Sundin A, Mjoeberg B. No recirculation after open cancellous bone grafting: a case examined by positron emission tomography. Clin Positron Imaging 2000;3(1):41–43

16. Berding G, Schliephake H, van den Hoff J, Knapp WH. Assessment of the incorporation of revascularized fibula grafts used for mandibular reconstruction with F-18-PET. Nuklearmedizin 2001;40:51–58

17. Brenner W, Kampen WU, Müller H, et al. F-18 fluoride PET in minipigs with defined disorders of bone metabolism [abstract]. J Nucl Med 2002;43:340P

18. DeGrado TR, Turkington TG, Williams JJ, et al. Performance characteristics of a whole-body PET scanner. J Nucl Med 1994;35:1398–1406

19. Lewellen TK, Kohlmeyer S, Miyaoka R, Schubert S, Stearns C. Investigation of the count rate performance of the General Electric Advance positron emission tomograph. IEEE Trans Nucl Sci 1995;42:1051–1057

20. Gjedde A. Calculation of cerebral glucose phosphorylation from brain uptake of glucose analogs in vivo: a re-examination. Brain Res 1982;257:237–274

21. Patlak CS, Blasberg RG, Fenstermacher JD. Graphical evaluation of blood-to-brain transfer constants from multiple-time uptake data. J Cereb Blood Flow Metab 1983;3:1–7

22. Piert M, Zittel TT, Machulla HJ, et al. Blood flow measurements with [15O]H$_2$O and [18F]fluoride ion PET in porcine vertebrae. J Bone Miner Res 1998;13:1328–1336

23. Piert M, Machulla HJ, Jahn M, et al. Coupling of porcine bone blood flow and metabolism in high-turnover bone disease measured by [15O]H$_2$O and [18F]fluoride ion positron emission tomography. Eur J Nucl Med Mol Imaging 2002;29:907–914

24. Weber WA, Ziegler SI, Thodtmann R, Hanauske AR, Schwaiger M. Reproducibility of metabolic measurements in malignant tumors using FDG PET. J Nucl Med 1999; 40:1771–1777

25. Brenner W, Vernon C, Muzi M, et al. Comparison of different quantitative approaches to [18F]-fluoride PET scans. J Nucl Med 2004; 45:in press